Tissue plasminogen activator regulates Purkinje neuron development and survival

Jianxue Li[a,1], Lili Yu[b], Xuesong Gu[c], Yinghua Ma[d], Renata Pasqualini[e], Wadih Arap[e], Evan Y. Snyder[f], and Richard L. Sidman[a,1]

Departments of [a]Neurology and [c]Medicine, Beth Israel Deaconess Medical Center, Harvard Medical School, Boston, MA 02215; [b]Department of Anatomy and Neurobiology, Boston University Medical School, Boston, MA 02118; [d]Department of Neurology and Neuroscience, Weill Medical College of Cornell University, New York, NY 10065; [e]David H. Koch Center, the University of Texas M. D. Anderson Cancer Center, Houston, TX 77030; and [f]Program in Stem Cell and Regenerative Biology, Sanford-Burnham Medical Research Institute, La Jolla, CA 92037

Contributed by Richard L. Sidman, March 29, 2013 (sent for review January 18, 2013)

The cerebellar cortex is centrally involved in motor coordination and learning, and its sole output is provided by Purkinje neurons (PNs). Growth of PN dendrites and their major synaptic input from granule cell parallel fiber axons takes place almost entirely in the first several postnatal weeks. PNs are more vulnerable to cell death than most other neurons, but the mechanisms remain unclear. We find that the homozygous nervous (*nr*) mutant mouse's 10-fold–increased cerebellar tissue plasminogen activator (tPA), a part of the tPA/plasmin proteolytic system, influences several different molecular mechanisms, each regulating a key aspect of postnatal PN development, followed by selective PN necrosis, as follows. (*i*) Excess endogenous or exogenous tPA inhibits dendritic growth in vivo and in vitro by activating protein kinase Cγ and phosphorylation of microtubule-associated protein 2. (*ii*) tPA/plasmin proteolysis impairs parallel fiber-PN synaptogenesis by blocking brain-derived neurotrophic factor/tyrosine kinase receptor B signaling. (*iii*) Voltage-dependent anion channel 1 (a mitochondrial and plasma membrane protein) bound with kringle 5 (a peptide derived from the excess plasminogen) promotes pathological enlargement and rounding of PN mitochondria, reduces mitochondrial membrane potential, and damages plasma membranes. These abnormalities culminate in young *nr* PN necrosis that can be mimicked in wild-type PNs by exogenous tPA injection into cerebellum or prevented by endogenous tPA deletion in *nr:tPA*-knockout double mutants. In sum, excess tPA/plasmin, through separate downstream molecular mechanisms, regulates postnatal PN dendritogenesis, synaptogenesis, mitochondrial structure and function, and selective PN viability.

plasma membrane integrity | postnatal development | spinocerebellar ataxia | synaptic ultrastructure

In the cerebellar cortex, the unusually large, highly active Purkinje neurons (PNs) are the main target of inputs and provide the sole output, participating in motor coordination and learning. PN dendrites are elaborately branched in the sagittal plane across the molecular layer (1). Closely packed parallel fiber (PF) axons of granule cell neurons, oriented transversely, collectively form more than 100,000 excitatory glutamatergic synapses on dendritic spines of each of the approximately 200,000 total PNs; PF axons individually form few synapses, commonly only one, on almost each of a few hundred PNs in a linear series (2). Many fundamental concepts of modern neuroscience have been established by study of PNs (3), because their cell bodies and dendrites are readily and vividly accessible in vivo and in vitro (4). PNs are more susceptible than most neurons to degeneration in a variety of disorders, including several of the more than 30 known spinocerebellar ataxias (5), as well as some cases of fetal and adult chronic alcohol syndromes, paraneoplastic diseases, lysosomal storage diseases, autism spectrum disorders, and Alzheimer's disease (6–8). Although the causal gene in many of the heritable ataxias now has been identified, the basis for the PN defects remains almost entirely undefined (6). Therefore, molecular regulators of PN development and survival merit elucidation.

The mouse autosomal recessive nervous (*nr*) mutation features ~60% PN loss during postnatal days 21–35 (P21–35), which is most severe in the lateral hemispheres of the cerebellum (9, 10), with some ongoing PN degeneration for months thereafter (11). The *nr* gene maps to a 1.4-cM region of mouse chromosome 8 between the D8Rck1 and D8Mit3 markers (12) but has not been cloned. We previously obtained evidence suggesting that a 10-fold increase in a serine protease, tissue plasminogen activator (tPA), in postnatally developing cerebellum may be the trigger for young PN degeneration (13, 14). Both PNs (15) and granule cell neurons (16) express tPA and its substrate, plasminogen (17). tPA catalyzes the conversion of circulating plasminogen to plasmin and is best known as a clinically approved agent for dissolving fibrinolytic blood clots in acute ischemic strokes (18). tPA also is an upstream regulator of several critical cell-maintenance processes, including neurotrophic factor handling and perhaps mitochondrial function. However, the mechanisms whereby the tPA/plasmin system regulates development and degeneration of postnatal PNs are mostly unknown.

Although our earlier papers suggested a direct role of tPA in PN development and death (13, 14), only now do we have unequivocal evidence, from an approach combining single-cell gene profiling, quantitative ultrastructural analysis, cerebellar organotypic slice and dissociated PN cell culturing, injection of tPA into WT neonatal cerebellar cortex, lentiviral vector-based shRNA transduction, analysis of enzymatic dynamics, and dendritic tree quantification, that multiple molecular pathways downstream of

Significance

Cerebellar Purkinje neurons (PNs) strongly affect motor coordination and learning. PN study has contributed significantly to fundamental concepts of modern neuroscience. The present investigation defines distinctive molecular signaling pathways through which tissue plasminogen activator/plasmin-based proteolysis regulates postnatal PN dendrite development, synapse formation, mitochondrial morphology and function, and PN survival. These pathways involve differentially acting downstream constituents, including protein kinase Cγ, brain-derived neurotrophic factor, and a voltage-dependent anion channel. The metabolic mechanisms established here may apply to the development and degeneration of PNs and additional types of neurons in many animal and human brain diseases in which PNs are notably vulnerable.

Author contributions: J.L., R.P., W.A., E.Y.S., and R.L.S. designed research; J.L., L.Y., X.G., and Y.M. performed research; J.L., L.Y., R.P., W.A., E.Y.S., and R.L.S. analyzed data; and J.L., R.P., W.A., E.Y.S., and R.L.S. wrote the paper.

The authors declare no conflict of interest.

Freely available online through the PNAS open access option.

[1]To whom correspondence may be addressed. E-mail: jli7@bidmc.harvard.edu or richard_sidman@hms.harvard.edu.

This article contains supporting information online at www.pnas.org/lookup/suppl/doi:10.1073/pnas.1305010110/-/DCSupplemental.

Downloaded at Palestinian Territory, occupied on December 16, 2021

www.manaraa.com

tPA/plasmin-based proteolysis affect postnatal PN development and degeneration. Excess tPA arising endogenously in *nr* homozygotes or exogenously by sustained cerebellar injection of tPA in WT mice (*i*) mediates underdevelopment of PN dendrites through protein kinase Cγ (PKCγ) activation and microtubule-associated protein 2 (MAP2) phosphorylation, (*ii*) impairs the formation of PF–PN synapses via reduced brain-derived neurotrophic factor/tyrosine receptor kinase B (BDNF/TrkB) signaling, and (*iii*) increases binding of kringle 5, a plasminogen catabolite peptide, to voltage-dependent anion channel 1 (VDAC1), leading to unusual changes in mitochondrial morphology and function and loss of cell membrane integrity, triggering selective necrosis of PNs. Importantly, deletion of endogenous tPA in *nr;tPA*$^{-/-}$ double mutants protects young *nr* PNs from these anomalies, whereas exposure of WT PNs in vivo or in vitro to excess tPA reproduces the abnormalities. These findings establish a causal relationship between the tPA proteolytic system and PN development and degeneration.

Results

tPA/Plasmin Proteolytic System in the Cerebellum. We first confirmed tPA content and expression in WT and *nr*-mutant mice with laser capture microdissection (LCM) to isolate single PNs and small groups of granule cells separately from P20 cerebellar cortices. With Affymetrix GeneChip array (Chip) and quantitative real-time PCR (qPCR) we identified both neuronal types as major producers of tPA and plasminogen (Fig. S1*A*). We found five- to 10-fold increased levels of tPA mRNA and protein, and two- to three-fold increased tPA fibrinolytic activity in P10 and P15 *nr* cerebella, compared with age-matched WT controls (Fig. S1 *B–D*); this increased activity occurred 4–9 d or longer before the onset of PN degeneration. The excess tPA was distributed throughout the cerebellar cortex (Fig. S1 *E* and *F*) as well as in the cerebellar deep nuclei (Fig. S1 *G* and *H*).

Suppression of Dendritic Development by Excess tPA via PKCγ and MAP2. We next analyzed in detail the effect of increased tPA on the postnatal development of PN dendrites, a key requirement for the establishment of cerebellar circuitry (19). Excess tPA was injected into WT cerebella at P15, and dendritic growth was analyzed by confocal microscopy and dendrite quantification. Excess tPA resulted in a thinner cerebellar cortical molecular layer, and PNs had abnormally short dendritic stems and fewer dendritic branchlets, resembling age-matched *nr* cerebella and differing significantly from age-matched WT controls (Fig. 1 *A–D*). In contrast, no obvious alterations were seen in the morphology of granule cells, molecular layer interneurons, oligodendrocytes, or Bergmann radial processes of the Golgi epithelial cell astrocytes (Fig. S2). Thus, excess tPA inhibits dendritogenesis of *nr* PNs during the normal postnatal period of cerebellar development.

tPA can activate PKC (20). Of the 11 members of the PKC family, PKCγ is prominently expressed in cerebellar PNs (21) and is a regulator of PN dendritic growth (22). With LCM, Chip, and qPCR, we verified that PKCγ mRNA was 100- to 1,000-fold higher in PNs than in granule cells in P20 cerebellar cortices (Fig. 1*E*). Although PKCγ protein levels in PNs did not differ among P15 WT, *nr*, and tPA-injected samples (Fig. 1 *F* and *G*), the PKC substrate, myristoylated alanine-rich C kinase substrate (MARCKS), was highly phosphorylated in P15 *nr* and tPA-injected WT cerebella as compared with untreated WT controls (Fig. 1*H*). These results suggest that PKCγ activation by excess endogenous or exogenous tPA mediates abnormal dendritic growth of young *nr* PNs.

To test this possibility directly, we set up cerebellar slices and dissociated cell cultures in which cells came to resemble postnatal PNs in vivo by developing dendritic branchlets through two successive, tightly regulated stages (23–25). In the first postnatal week (the normal "early" stage), bipolar fusiform PNs retract their primitive processes and extend numerous short perisomatic protrusions. In the second postnatal week (the normal "late" stage),

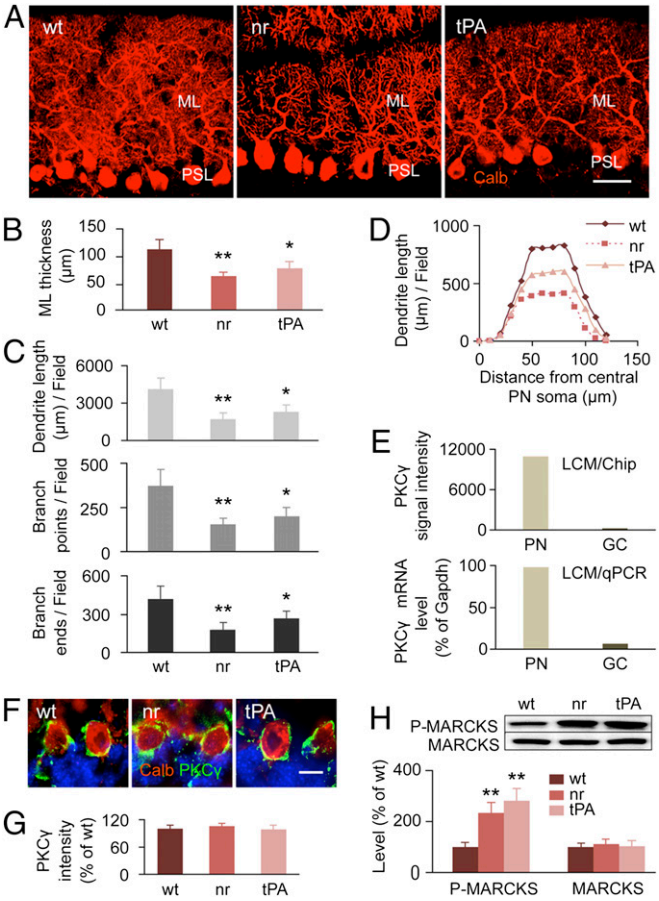

Fig. 1. tPA regulates PN dendritic development and PKCγ activity in the cerebellar cortex. (*A*) Calbindin-D-28K (Calb)-stained PN dendrites (red) in the molecular layer (ML) were decreased in P15 *nr* (labeled "nr") and tPA-injected (1 μg/μL at P10) WT (labeled "tPA") cerebellar cortices as compared with untreated WT controls (labeled "WT"). PSL, PN soma layer. (Scale bar: 20 μm.) (*B*) Thickness of the molecular layer was reduced significantly in the P15 *nr* and tPA-injected WT mice compared with the untreated WT group. Values represent means ± SD, $n = 4–6$ for each group. $^*P < 0.05$, $^{**}P < 0.01$ compared with WT control. (*C*) Dendrite length, branch points, and branch ends of PNs in the above samples (also see Fig. S3*B*). Values represent means ± SD, $n = 6–8$ for each group. $^*P < 0.05$, $^{**}P < 0.01$ compared with WT control. (*D*) Sholl analysis of the total length of PN dendrites within each concentric circle (0–10 μm, 10–20 μm, … 110–120 μm) in the above samples. The area under each curve represents an average value of the total PN dendrite length in each group. Peak values correlated positively with dendritic density. (*E*) PKCγ mRNA at P20, detected by PKCγ signal intensity and mRNA level, were expressed predominantly in P20 WT PNs, rather than in granule cells (GC). (*F*) Representative images of PKCγ protein (green) appeared similar in P15 WT, *nr*, and tPA-injected PNs. Cell nuclei were DAPI-stained (blue). (Scale bar: 10 μm.) (*G*) PKCγ protein intensity also was similar in PNs of P15 WT, *nr*, and tPA-injected mice. Values represent means ± SD, $n = 4–6$ for each group. (*H*) Protein levels of phosphorylated MARCKS (P-MARCKS) were increased significantly in P15 *nr* and tPA-injected WT cerebella compared with WT controls. Values represent means ± SD, $n = 4–6$ for each group. $^{**}P < 0.01$ compared with WT control.

PNs form a primary dendrite and undergo rapid dendritic elongation and branching restricted to the sagittal plane (25). We treated cerebellar cell cultures at 2–7, 8–14, or 8–21 d in vitro (DIV) and quantified PN dendrites at 7, 14, or 21 DIV. We found that tPA, tPA+plasminogen (tPA+PL), or a PKC agonist (phorbol 12-myristate 13-acetate) did not change the dendritic trees of PNs at the early stage (2–7 DIV) (Fig. S3) but significantly suppressed total dendrite length, branch points and ends, and dendrite tree distribution at the late stage (8–14 DIV) (Fig. 2 *A–C*), as is consistent

PNAS PLUS
NEUROSCIENCE
Downloaded at Palestinian Territory, occupied on December 16, 2021
www.manaraa.com

with roles of other extrinsic regulators of PN dendritic development (4, 25). Conversely, the PKC inhibitor (Gö6976) and PKCγ shRNA efficiently rectified PN dendrites in tPA+PL-treated cerebellar cell cultures (Fig. 2 *A*–*C*), whereas two other downstream targets of the tPA/plasmin proteolytic system, BDNF and neurotrophin 3 (NT3), individually had no effect. Also, PKC activity, evaluated by the phosphorylated MARCKS (P-MARCKS) level (Fig. 2*D*), was negatively correlated with dendritic growth of cultured PNs (Fig. 2*A*), further indicating a role of PKC activity in regulating PN dendrites.

MAPs promote tubulin assembly and form cross-bridging microtubules. MAP2 is expressed prominently and plays a role in the growth of PN dendrites (26, 27). In addition, MAP phosphorylation is associated with dendritic remodeling (28), and site-specific phosphorylation by PKC can inhibit the assembly-promoting activity of certain MAPs (29). Therefore, we analyzed MAP2 phosphorylation levels upon inhibition of dendrite growth. tPA+PL or PKC agonist significantly increased MAP2 phosphorylation, and the PKC inhibitor prevented MAP2 phosphorylation in cerebellar cell cultures (Fig. 2*E*). The concept that excess tPA suppresses development of *nr* PN dendrites via PKCγ activation and MAP2 phosphorylation is considered further in *Discussion*.

Abnormal Synaptogenesis Induced by Excess tPA via BDNF/TrkB Signaling. Because PN dendrites are critical postsynaptic targets, each receiving far more synaptic inputs than are found on dendrites of any other type of neuron, we explored the effects of

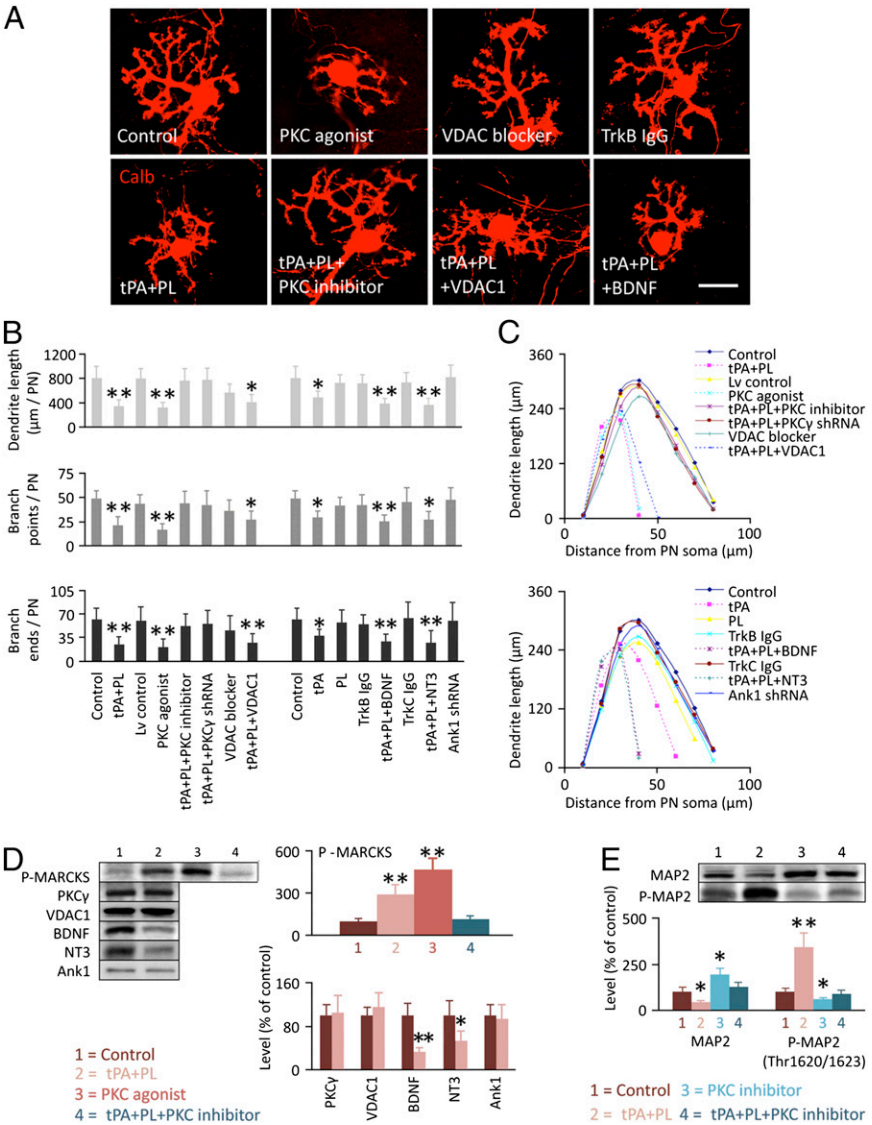

Fig. 2. tPA and PKCγ mediate PN dendritic growth in cerebellar dissociated cell cultures. (*A*) Treatment with tPA+PL (20+5 μg/mL at 8–14 DIV) or PKC agonist, rather than a VDAC blocker or TrkB IgG, inhibited calbindin-D-28K (Calb)-stained PN dendrites in cerebellar cell cultures at 14 DIV. PKC inhibitor, rather than VDAC1 or BDNF, rectified the inhibitory effect of tPA+PL treatment. (Scale bar: 20 μm.) (*B*) Quantification of dendrite length, branch points, and branch ends of PNs in the above samples (also see Fig. S3*B*). Lv, lentiviral vector. Values represent means ± SD, $n = 6$–10 for each treatment. $^{*}P < 0.05$, $^{**}P < 0.01$ compared with control. (*C*) Sholl analysis of total length of PN dendrites in the above samples, as in Fig. 1*D*. Peak values correlated positively with dendritic density. (*D* and *E*) Effects of tPA+PL, a PKC agonist, or a PKC inhibitor, respectively, on PKC activity (P-MARCKS level) and on the levels of several important proteins (*D*) and of MAP2 and phosphorylated MAP2 (P-MAP2) (*E*) in the above samples. Treatment with tPA+PL or PKC agonist increased phosphorylation of MARCKS and MAP2 and suppressed PN dendritic growth, whereas the PKC inhibitor rectified these effects of tPA+PL treatment. Values represent means ± SD, $n = 6$–8 for each treatment. $^{*}P < 0.05$, $^{**}P < 0.01$ compared with control.

Downloaded at Palestinian Territory, occupied on December 16, 2021
www.manaraa.com

excess tPA/plasmin proteolysis on PN synaptogenesis. Excitatory PF–PN synapses are composed of granule cell axon presynaptic components (filled with numerous round, loosely packed vesicles) in contact with PN dendritic spines (featuring a prominent postsynaptic density at the spine surface) (1, 2), which are most numerous in the outer region of the cerebellar molecular layer. By quantitative transmission electron microscopy and immunohistochemistry, we found significant decreases in the number of PF–PN synapses, in their number of presynaptic vesicles, and in postsynaptic density length (Fig. 3 *A* and *B*), as well as reduction of a major postsynaptic protein marker, postsynaptic density 95 (PSD95) (Fig. S4) in P15 *nr* and tPA-injected WT cerebella as compared with untreated WT controls. Thus, excess tPA also induces abnormal PN synaptogenesis.

The neurotrophins BDNF and NT3 activate Trk receptors and are known to modulate cerebellar plasticity and PF–PN synapses (30). BDNF and NT3 also are downstream of tPA, so we speculated that they may mediate the effect of excess tPA on PN synaptogenesis. With LCM, Chip, and qPCR, we identified that in P20 cerebella granule cells are the dominant producers of BDNF, whereas PNs contain relatively more TrkB receptors (Fig. 3*C*). Upon checking whether cerebellar neurotrophic factors are substrates of the tPA/plasmin proteolytic system, we found that excess tPA of endogenous or exogenous origin caused a reduction in BDNF and NT3 protein levels but not in the levels of their receptors (TrkB and TrkC, respectively) or of the nerve growth factor receptor, p75, in P15 *nr* and tPA-injected WT cerebella (Fig. 3 *D–F* and Fig. S5). We therefore hypothesized that defective neurotrophic signaling caused by excess tPA might impair young *nr* PF–PN synapses.

To test whether such a decrease in BDNF/TrkB and/or NT3/TrkC signaling caused by excess tPA/plasmin proteolysis reduces PN synaptogenesis, we examined PN postsynaptic sites with the postsynaptic protein marker PSD95 and dendritic branchlets by staining with calbindin in cerebellar cell cultures. We found that tPA+PL or TrkB IgG (a BDNF/TrkB signaling inhibitor) significantly down-regulated PSD95 mRNA expression. In contrast, TrkC IgG (an NT3/TrkC signaling inhibitor) or a PKC agonist had no effect. Importantly, addition of exogenous BDNF, but not NT3, a PKC inhibitor, or PKCγ shRNA, prevented the down-regulation of PSD95 mRNA induced by tPA+PL (Fig. 4*A*). Also, TrkB IgG, but not TrkC IgG or a PKC agonist, imitated the inhibitory effect of excess tPA/plasmin proteolysis on PSD95 protein levels at postsynaptic sites. In addition, both tPA and a PKC agonist inhibited the intensity of calbindin staining at dendritic branchlets of cultured PNs (Fig. 4 *B* and *C*). The tPA-induced reduction in calbindin staining was rescued with a PKC inhibitor (Fig. 4 *B* and *C*). Thus, reduced BDNF/TrkB signaling, rather than NT3/TrkC signaling or PKC activity, mediates the abnormal synaptogenesis of *nr* PNs caused by excess tPA.

Mitochondrial Changes Mediated by VDAC1 Bound with Plasminogen Kringle 5. Mitochondria play crucial roles in cellular bioenergetics, signaling transduction, organelle intercommunication, and cell proliferation, differentiation, survival, and programmed death (31–33). Unusual shape and size of mitochondria are exceptional pathological hallmarks in neurons but occur in all young *nr* PNs and correlate with their later selective necrotic cell death. Their regulation and role in the *nr* phenotype have been unresolved for decades (9–11, 34). We found in the present study that after injection of excess tPA into P15 WT mouse cerebellum in vivo, PNs contained enlarged rounded mitochondria similar to those in age-matched *nr* samples (Fig. 5 *A* and *B*). Because VDAC in both the mitochondrial outer membrane and the cellular plasma membrane (35) (Fig. 5*C*) is a gatekeeper regulating cell life and death (32, 36), we explored whether VDAC affects *nr* PN degeneration. Of the three VDAC family members, VDAC1 is the most abundant, and its mRNA was prominent in P20 WT PNs and granule cells (Fig. 5*D*). Excess endogenous or exogenous tPA induced redistribution

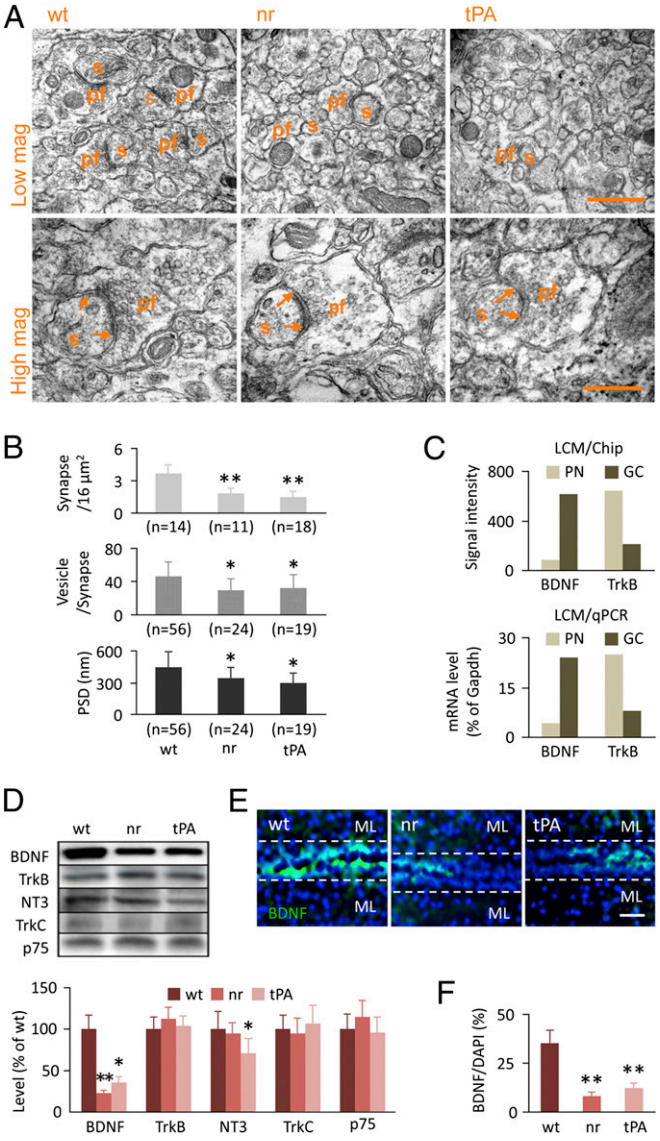

Fig. 3. tPA affects the PN synaptic ultrastructure and the BDNF level in the cerebellar cortex. (*A*) Transmission electron microscopy disclosed ultrastructural changes in asymmetric PF–PN synapses in the distal part of the molecular layer of P15 *nr* and tPA-injected (1 μg/μL at P10) WT cerebellar cortices compared with untreated WT controls. The heavily stained segment between two arrows shows the postsynaptic density. High mag, high magnification; Low mag, low magnification; pf, parallel fiber presynaptic terminals; s, PN dendrite spine. (Scale bars: 1,000 nm for low magnification; 500 nm for high magnification.) (*B*) Synapse number, presynaptic vesicle number, and postsynaptic density (PSD) length of the above samples were decreased significantly in P15 *nr* and tPA-injected groups compared with the untreated WT group. Values represent means ± SD, n = 11–56 for each group. *$P < 0.05$, **$P < 0.01$ compared with control. (*C*) BDNF (ligand) mRNA was found mainly in granule cells (GC), whereas TrkB (receptor) mRNA was found mainly in the PNs of P20 WT mouse cerebellum, detected by LCM/Chip (signal intensity) and LCM/qPCR (mRNA level). (*D*) As evident in the gel bands (*Upper*) and the bar graph (*Lower*), the protein level of BDNF, rather than TrkB, was decreased in P15 *nr* and tPA-treated cerebella as compared with WT controls. Values represent means ± SD, n = 4–6 for each group. *$P < 0.05$, **$P < 0.01$ compared with control. (*E* and *F*) Representative images (*E*) and quantification (*F*) showed that BDNF distribution (green in *E*) was reduced in the small residual external granular layer (shown in two apposed lobules, between the dashed lines) of P15 *nr* and tPA-treated cerebella as compared with WT controls. ML, molecular layers of the apposed lobules at the top and bottom of the images. Cell nuclei were stained with DAPI (blue). Values represent means ± SD, n = 4–6 for each group. **$P < 0.01$ compared with control. (Scale bar: 20 μm.)

PNAS PLUS
NEUROSCIENCE
Downloaded at Palestinian Territory, occupied on December 16, 2021
www.manaraa.com

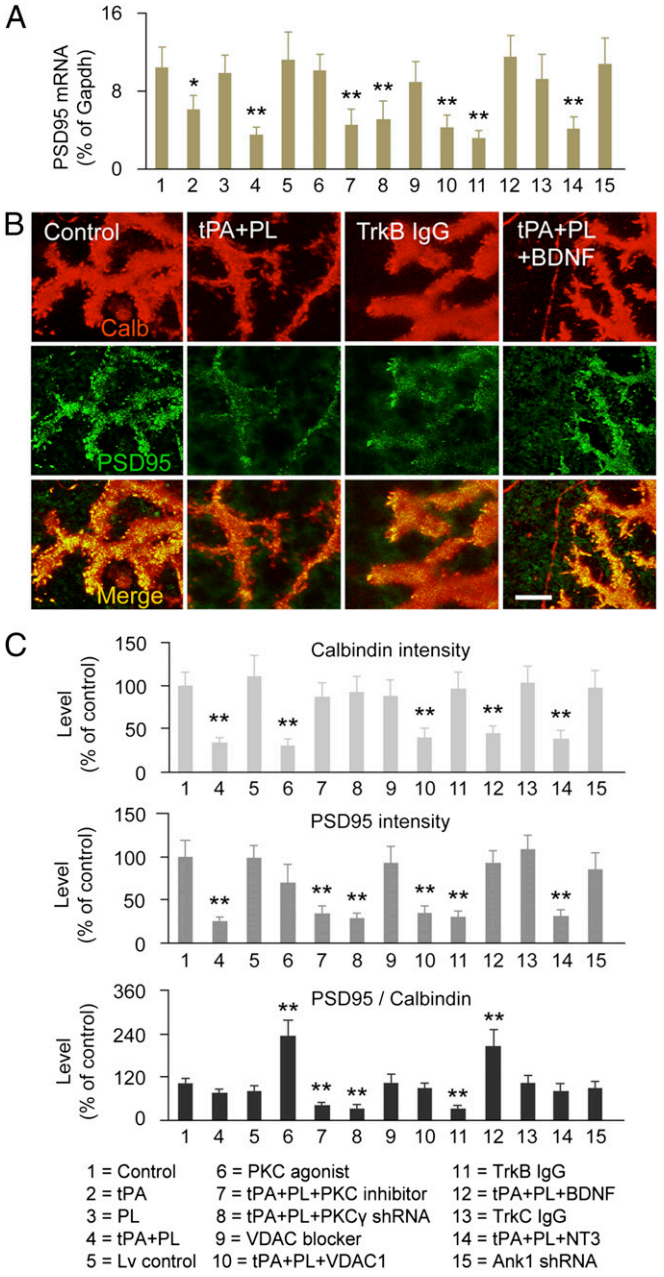

Fig. 4. tPA and BDNF regulate PN synapse formation in cerebellar dissociated cell cultures. (*A*) qPCR data (designations for each number along the *x*-axis are listed at the bottom of the figure) showed that tPA+PL (#4) (20+5 μg/mL at 8–14 DIV) or TrkB IgG (#11) significantly reduced postsynaptic density 95 (PSD95) mRNA levels at 14 DIV. BDNF (#12), rather than PKC inhibitor (#7) or VDAC1 (#10), rectified the inhibitory effect of tPA+PL treatment. Lv, lentiviral vector. Values represent means ± SD, n = 6–8 for each treatment. $^{*}P < 0.05$, $^{**}P < 0.01$ compared with control. (*B*) Representative images of calbindin-D-28K (Calb)-stained PN dendritic branchlets (red) and PSD95-stained postsynaptic sites (green) showed that tPA+PL or TrkB IgG decreased PSD95 staining in dissociated cell cultures at 14 DIV and that the addition of BDNF to tPA+PL corrected the concentration of PSD95-stained postsynaptic sites, although, as expected, it did not reverse the tPA+PL-induced reduction in dendritic branchlets. (Scale bar: 5 μm.) (*C*) Quantification of the intensities of Calb and PSD95 staining (from samples in *B*) and of the PSD95 (postsynaptic site)/Calb (dendritic branchlet) ratio supported the notion that blockage of BDNF/TrkB signaling by excess tPA/plasmin proteolysis inhibited formation of PF–PN synapses in vitro. Values represent means ± SD, n = 6–10 for each treatment. $^{**}P < 0.01$ compared with control.

of VDAC1 (Fig. 5 *E* and *F*) and cytochrome *c* oxidase (a mitochondrial inner membrane marker) (Fig. S6), with a markedly increased concentration in PN somata (where the enlarged mitochondria concentrate) and a decrease in the molecular layer (where mitochondria are markedly reduced), suggesting that perhaps the enlarged mitochondria marked by VDAC1 could not migrate into distal small-caliber parts of the dendritic tree. Plasminogen contains structural domains termed kringle 1–4 and kringle 5 that are peptides produced by proteolytic processing. VDAC is the receptor for plasminogen kringle 5 (37). We found that kringle 5 levels were increased in P15 *nr* and tPA-injected

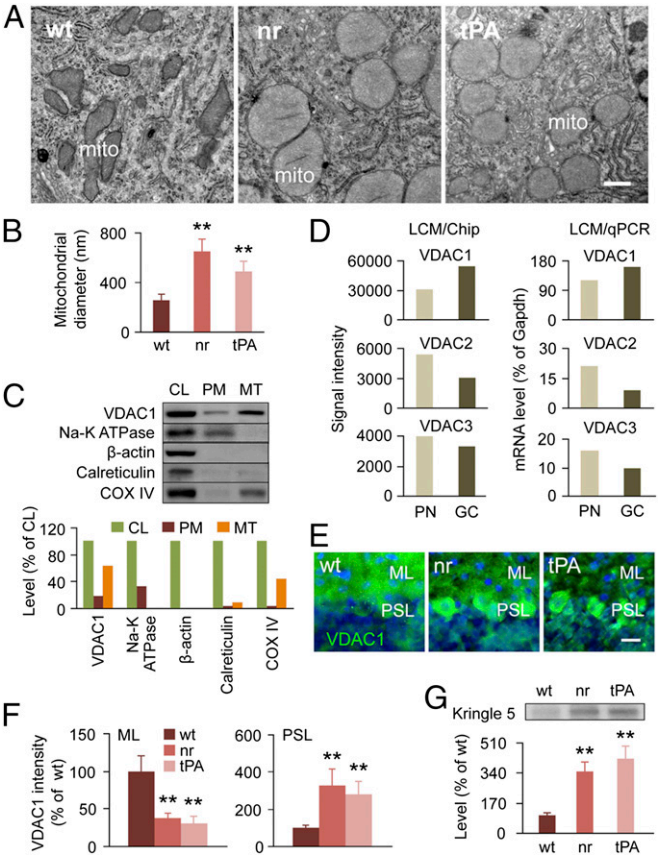

Fig. 5. tPA influences PN mitochondria and VDAC in cerebellar cortex. (*A* and *B*) Transmission electron microscopy showed huge, round mitochondria (*A*) with increased diameters (*B*) in P15 *nr* and tPA-injected (5 μg/μL at P10) WT cerebellar PNs compared with untreated WT controls. mito, mitochondria. Values represent means ± SD, n = 20 mitochondria for each group. $^{*}P < 0.05$, $^{**}P < 0.01$ compared with control. No significant difference was seen between *nr* and tPA-injected PNs. (Scale bar: 400 nm.) (*C*) Intracellular distribution of VDAC1 in both mitochondria (MT) and plasma membrane (PM) fractions of the cell lysate (CL). Protein levels of VDAC1 and other organelle markers were measured in the cell lysate, plasma membrane, and mitochondria of cultured PNs. Na-K ATPase, a cell membrane marker, was detected in the plasma membrane. Calreticulin, an endoplasmic reticulum marker, was not detected in plasma membrane or mitochondria; cyclooxygenase IV (COX IV), a mitochondrial inner membrane marker, was found in mitochondria. The results verified the high purity of the cellular fractions and the presence of VDAC1 in both mitochondria and plasma membrane. (*D*) VDAC1 mRNA was five- to10-fold greater than VDAC2 or VDAC3 mRNA in PNs and granule cells (GC) in P20 WT mice as detected by LCM/Chip and LCM/qPCR. (*E* and *F*) Representative images (*E*) and quantification (*F*) showed that VDAC1 distribution (green in *E*) was decreased in the molecular layer (ML) but was increased in the PN soma layer (PSL) of P15 *nr* and tPA-injected cerebellar cortices as compared with WT controls. Cell nuclei were stained with DAPI (blue). Values represent means ± SD, n = 4–6 for each group. $^{**}P < 0.01$ compared with control. (Scale bar: 15 μm.) (*G*) Plasminogen kringle 5 levels were increased significantly in P15 *nr* and tPA-treated cerebella compared with WT controls. Values represent means ± SD, n = 4–6 for each group, $^{**}P < 0.01$ compared with control.

Downloaded at Palestinian Territory, occupied on December 16, 2021
www.manaraa.com

WT cerebellar cortices, as compared with untreated WT controls (Fig. 5*G*), and that kringle 5, rather than kringle 1–4, could bind to VDAC1 in cultured PNs (Fig. S6). We hypothesized that kringle 5-bound VDAC1 in young *nr* PNs before the onset of cell death might mediate mitochondrial malfunction triggered by excess tPA.

To test this hypothesis, we explored the effects of excess tPA on mitochondrial function in cerebellar cell and PN cultures. Mitochondrial membrane potentials (ΔΨm) and voltage-gated ion channels form a dynamic feedback loop (38). We found that tPA+PL or a VDAC blocker (cyclosporine A), significantly reduced mitochondrial ΔΨm in cultured PNs (Fig. 6 *A* and *B*), and this reduction was concurrent with the presence of enlarged mitochondria (Fig. 6 *C* and *D*), similar to PN mitochondria in young *nr* cerebella in vivo (Fig. 5 *A* and *B*). In contrast, a PKC agonist, TrkB IgG or TrkC IgG, had no such effect (Fig. 6 *B* and *D*). The changes in mitochondrial morphology and function were associated further with the reduction of ATP in vitro (Fig. 6*E*). The addition of VDAC1, but not the inhibition of PKC activity or enhancement of neurotrophic signaling, protected PN mitochondria from the pathological changes triggered by tPA+PL or VDAC blocker (Fig. 6). These results verify that excess tPA has abnormal effects on mitochondrial morphology and function in *nr* PNs, likely acting through the binding of plasminogen kringle 5 to its VDAC1 receptor (37).

Cell Death Caused by Excess tPA via Abnormal Mitochondria and Plasma Membrane. Cell death in general occurs by apoptotic, necrotic, autophagic, or additional mixed mechanisms (39). Like the extensive degeneration of PNs in young *nr*-mutant mice, we found selective death of PNs in P20 tPA-injected WT cerebella (Fig. 7 *A* and *B*), which was independent of caspase 3 activity (Fig. 7 *C* and *D*). Also, in cerebellar cell and PN cultures, tPA+PL or a VDAC blocker led to increased PN death at 21 DIV (Fig. 7 *E* and *F*), although not at 14 DIV (Fig. S7). The addition of VDAC1 prevented PN death triggered by excess tPA/plasmin proteolysis (Fig. 7 *E* and *F*), but inhibition of PKC activity or enhancement of neurotrophic signaling had no effect. Moreover, most of these results in primary cell cultures were reproduced in cerebellar organotypic slice cultures (Fig. S7). We did not find caspase 3/7-dependent apoptosis (Fig. 7*G*) but did detect lactate dehydrogenase leakage—a sign of plasma membrane damage—in cerebellar cell cultures treated with tPA+PL (Fig. 7*H*). Statistical analyses further suggest that (*i*) changes in the integrity of the cell plasma membrane, where VDAC1 also is located (Fig. 5*C*) (35), may contribute to PN degeneration (Fig. 7*I*); (*ii*) VDAC-associated mitochondrial ΔΨm correlated positively and mitochondrial diameter correlated negatively with PN viability (Fig. 7*J*); and (*iii*) neither PKC-associated dendritic underdevelopment nor BDNF-associated synaptic defect correlated significantly with PN death (Fig. S7). Based on these results, we propose that mitochondrial malfunction and plasma membrane damage mediate selective necrosis of *nr* PNs, triggered by VDAC1 binding of plasminogen kringle 5 generated by excess tPA/plasmin proteolysis.

To test whether endogenous tPA deletion would prevent *nr* PN death, we mated BALB/cByJ-*nr* and C57BL/6J-*tPA*$^{-/-}$ mice and in subsequent generations produced *nr;tPA*$^{-/-}$ double mutants. We identified genotypes of individual *nr* mice before the development of phenotypic abnormalities by detecting D8Mit marker polymorphisms on either side of the known position of *nr* on chromosome 8, even though the *nr* gene itself has not been cloned. The intercrossed hybrid homozygous *nr* mice showed the same phenotype (massive PN loss and ataxia in the fourth postnatal week) as the homozygous BALB/cByJ-*nr* mutants, indicating no detected modification of the *nr* phenotype by input of alleles from the C57BL/6J strain.

In contrast to these identical behavioral and pathological phenotypes in near-isogenic BALB/cByJ-*nr* and the hybrid *nr* mice, the levels of tPA mRNA, protein, and fibrinolytic activity were undetectable or extremely low in P10 and P15 *tPA*$^{-/-}$ and *nr;tPA*$^{-/-}$ double-mutant mice (Fig. S1), comparable to similarly undetectable brain tPA by a different analytical method in the *tPA*$^{-/-}$ mouse

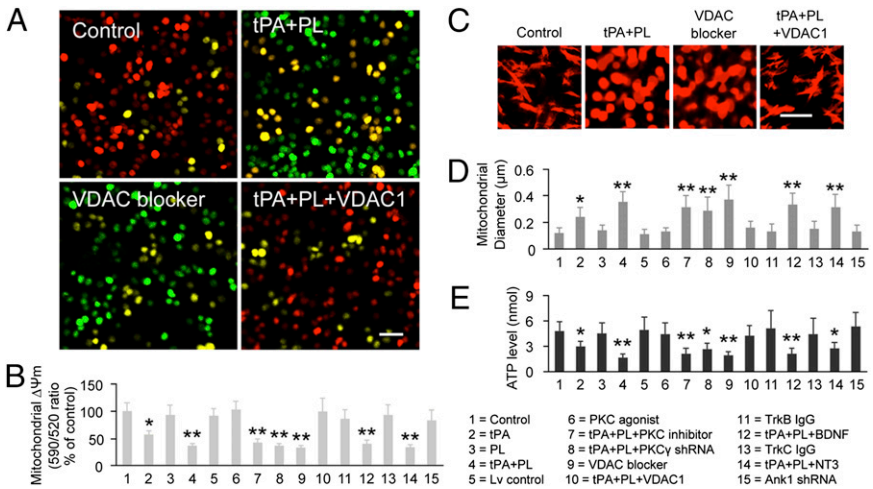

Fig. 6. tPA and VDAC regulate PN mitochondrial morphology and function in cerebellar dissociated cell cultures. (*A*) Representative images of JC-10 dye-stained PN cultures showed normal ΔΨm (red) in untreated control cultures and abnormally reduced ΔΨm (green) in cultures treated with tPA+PL (100+25 μg/mL) at 8–14 DIV or with VDAC blocker at 14 DIV. Reversible formation of JC-10 aggregates was based on membrane polarization that caused shifts in emitted light from 520 nm (JC-10 monomer emission) to 570 nm (JC-10 aggregate emission). In normal cells, JC-10 concentrated in the mitochondrial matrix where it formed red fluorescent aggregates at high Δψm, but in apoptotic and necrotic cells with low mitochondrial Δψm JC-10 diffused from mitochondria in monomeric form and fluoresced green. (Scale bar: 50 μm.) (*B*) Quantification confirmed that tPA+PL or VDAC blocker significantly decreased ΔΨm, whereas the addition of VDAC1 to tPA+PL corrected ΔΨm. Numbers under the *x*-axis are defined at the bottom of the figure. Lv, lentiviral vector. Values represent means ± SD, $n = 6$–10 for each treatment. $^{*}P < 0.05$, $^{**}P < 0.01$ compared with control. (*C* and *D*) Mitochondrial morphology (*C*) and diameters (*D*) confirmed that tPA+PL or VDAC blocker induced mitochondria to become huge and round, as seen here in CMXRos-stained PNs at 14 DIV. Values represent means ± SD, $n = 20$ mitochondria. $^{*}P < 0.05$, $^{**}P < 0.01$ compared with control. (Scale bar: 2 μm.) (*E*) tPA+PL or VDAC blocker also significantly inhibited ATP levels in cultured PNs. Values represent means ± SD, $n = 6$–8 for each treatment. $^{*}P < 0.05$, $^{**}P < 0.01$ compared with control.

Downloaded at Palestinian Territory, occupied on December 16, 2021
www.manaraa.com

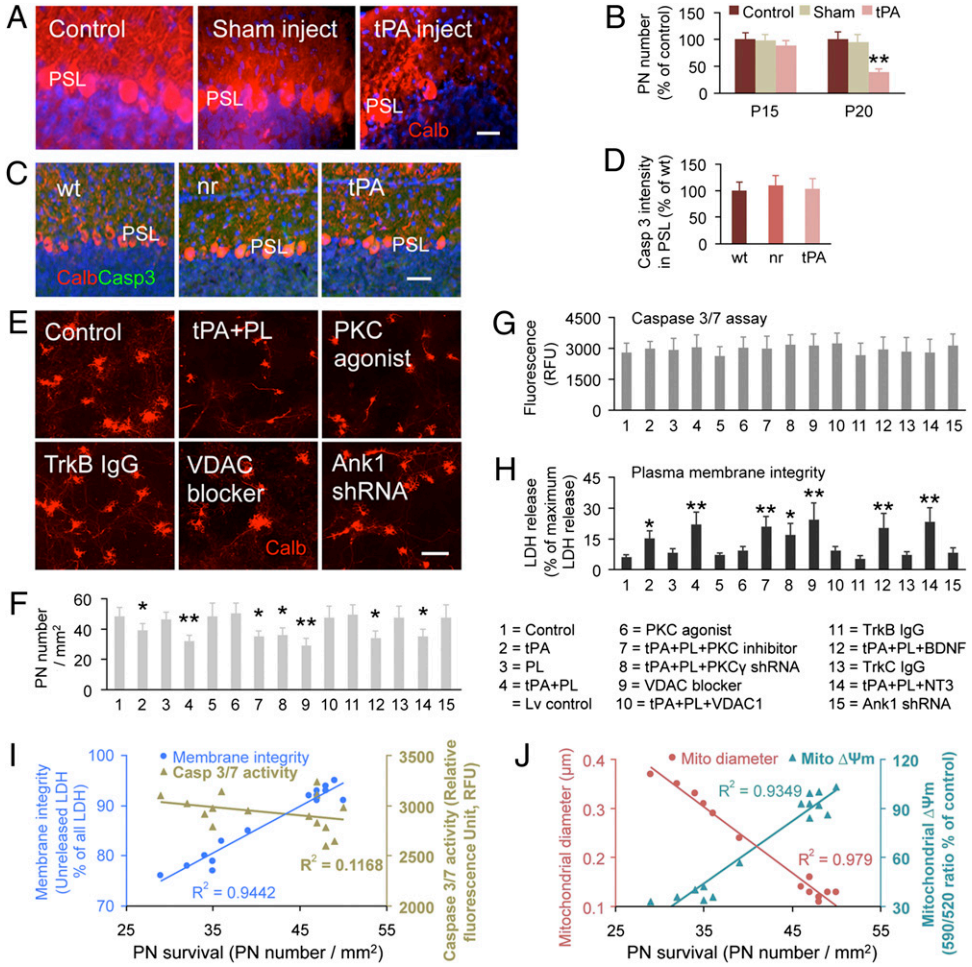

Fig. 7. tPA and VDAC mediate caspase 3/7-independent PN death. (*A* and *B*) Representative images (*A*) and quantification (*B*) showed reduced survival of calbindin-D-28K (Calb)-stained PNs (red in *A*) in P20 tPA-injected (5 μg/μL at P10) WT cerebellar cortex compared with untreated or sham-injected WT controls. Cell nuclei are stained with DAPI (blue). PSL, PN soma layer. Values represent means ± SD, $n = 4–6$ for each group. $*P < 0.05$, $**P < 0.01$ compared with control. (Scale bar: 15 μm.) (*C* and *D*) Representative images (*C*) and quantification (*D*) of Calb-stained (red) and caspase 3 (Casp3)-stained (green in *C*) sections showed no double-stained PNs in P20 WT, *nr,* or tPA-injected cerebellar cortices. Values represent means ± SD, $n = 6–8$ for each group. (Scale bar: 30 μm.) (*E* and *F*) Representative images (*E*) and quantification (*F*) of Calb-stained PNs (red in *E*) indicated that tPA+PL (100+25 μg/mL at 8–14 DIV) or VDAC blocker, rather than PKC agonist or TrkB IgG, increased PN death in cerebellar dissociated cell cultures at 21 DIV. Lv, lentiviral vector. Values represent means ± SD, $n = 6–8$ for each treatment. $*P < 0.05$, $**P < 0.01$ compared with control. (Scale bar: 50 μm.) (*G* and *H*) Quantification of caspase 3/7 activity (*G*) and plasma membrane integrity (LDH assay) (*H*) suggested that tPA+PL or VDAC blocker did not change the caspase 3/7 level but did increase LDH release in cerebellar cell cultures at 21 DIV. Values represent means ± SD, $n = 6–8$ for each treatment. $*P < 0.05$, $**P < 0.01$ compared with control. (*I*) Correlation analysis of plasma membrane integrity (positive correlation, $P < 0.01$) or caspase 3/7 activity (no correlation, $P > 0.05$) with PN survival. (*J*) Correlation analysis of ΔΨm (positive correlation, $P < 0.01$) or mitochondrial diameter (negative correlation, $P < 0.01$) with PN survival.

at an unstated age (40). In agreement with a previous report by others (41), we did not find PN death or ataxia in young or adult $tPA^{-/-}$ mice. Most importantly, the double mutants showed a significant reduction of PN death, as counted in all cerebellar cortical lobules, i.e., ∼20% and ∼50% PN loss, respectively, in P40 and P120 *nr;*$tPA^{-/-}$ mice, compared with 60% and 80% PN loss in P40 and P120 *nr* mice, respectively, on the BALB/cByJ × C57BL/6J background (Fig. 8 *A* and *B*). Also, P40 *nr;*$tPA^{-/-}$ mice displayed much better motor coordination, as measured by behavior on a rotarod, than did P40 *nr* mice (Fig. 8*C*). These results indicate that endogenous tPA deletion rescues many *nr* PNs (these surviving PNs contain normal mitochondria and maintain essentially normal motor coordination at P40), verifying excess tPA as the major contributor to *nr* ataxia. However, because tPA deletion did not completely rescue *nr* PNs, additional molecules likely are involved in the modest ongoing PN death in *nr* mice at ages older than P40 (42).

In summary, excess tPA/plasmin proteolysis affects the postnatal development of PN dendrites, the ultrastructure of PF–PN synapses, the morphology and function of PN mitochondria, and the survival of PNs in vivo (Table S1) and in vitro (Table S2) via differentially acting downstream constituents that include a kinase (PKCγ), a neurotrophin (BDNF), and a mitochondrial and plasma membrane channel (VDAC1) (Fig. 8*D*).

Discussion

Cerebellar tPA is normally present in young granule cells migrating inward across the molecular layers in the first two postnatal weeks and thereafter gradually becomes markedly reduced in these neurons as they mature in the internal granular layer (15). With combined LCM, Chip, qPCR, Western blot, fibrinolytic assay, and immunohistochemistry, we have quantified the distribution and activities of the tPA/plasmin proteolytic system specifically in young cerebellar PN somata and granule cells.

Postnatal development of PN dendrites and synapses is well known to occur through tightly regulated stages involving regression of cytoplasmic processes emerging from the cell body,

Downloaded at Palestinian Territory, occupied on December 16, 2021
www.manaraa.com

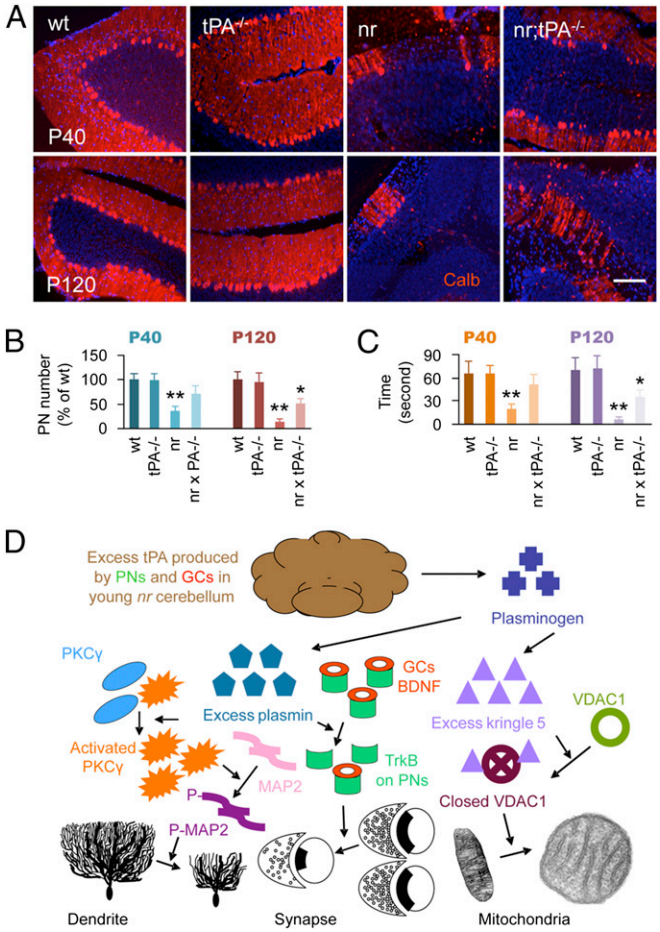

Fig. 8. Protection of *nr* PNs by tPA deletion and the proteolytic pathways controlling *nr* PN development. (*A–C*) Representative images (*A*) of calbindin-D-28K (Calb)-stained PNs (red in *A*), quantification in the sum of all cerebellar cortical lobules (*B*), and motor coordination behavior measured by rotarod test (*C*) in P40 and P120 WT, $tPA^{-/-}$ ($tPA^{-/-}$), *nr*, and $nr;tPA^{-/-}$ (double mutant) cerebellar cortices. The results indicated that deletion of endogenous tPA in $nr;tPA^{-/-}$ double mutants significantly increased PN survival and restored motor coordination behavior of *nr* mice. Values represent means ± SD, $n = 4–6$ for each group. $^{*}P < 0.05$, $^{**}P < 0.01$ compared with control. (Scale bar: 100 μm.) (*D*) Diagram summarizing our overall view of tPA-based proteolytic pathways controlling PN dendrite and synapse development and the mitochondrial pathology before necrosis. Excess tPA produced by PNs and granule cells (GCs) in young *nr* cerebella activates PKCγ and inactivates MAP2, inhibiting PN dendritic growth. Excess tPA/plasmin proteolysis degrades granule cell-derived BDNF, decreasing BDNF/TrkB signaling in PNs and in turn impairing the formation and structure of PF–PN synapses. Excess tPA increases binding of the plasminogen catabolite kringle 5 to VDAC1, and the modified VDAC1 further alters mitochondrial structure and function.

elongation of a primary dendritic stem, and extensive branching and maturation within the molecular layer (23–25). Here we identify PKCγ activation and BDNF/TrkB signaling as mediators, respectively, of dendritic growth and synapse formation of postnatally differentiating PNs.

PKCγ expression is very low at birth and peaks in the third postnatal week, concurrent with the impairment of *nr* PN dendritic development. tPA may be a PKC agonist (20). We now have shown that excess tPA originating endogenously (*nr* mutant) or exogenously (via tPA injection into cerebella of WT mice) does not change the net PKCγ level but does greatly stimulate PKCγ activity, as verified by increased MARCKS phosphorylation in vivo and in vitro. Because a PKC agonist inhibits dendritic growth, whereas a PKC inhibitor reduces MAP2 phosphorylation and restores dendritic growth that otherwise would be suppressed by tPA+PL treatment, it is likely that PKCγ activation by excess tPA negatively controls dendritic development in young *nr* PNs.

Levels of BDNF and TrkB in developing brains vary under different physiological and pathological conditions (43, 44). We find that granule cells are the predominant producers of BDNF, a ligand, whereas PNs are rich in its receptor, TrkB. Inositol 1,4,5-trisphosphate signaling controls the morphology and function of PF–PN synapses via BDNF (45, 46). In the present study, we found that excess tPA of endogenous or exogenous origin reduces granule cell BDNF, impairing PF–PN synaptic ultrastructure in vivo. Further, blockage of BDNF/TrkB signaling by a neutralizing TrkB IgG reduces the postsynaptic marker PSD95, whereas a BDNF supplement counteracts the deleterious role of tPA+PL on PSD95 in cultured PNs. Thus, BDNF degradation by excess tPA/plasmin proteolysis mediates abnormal PF–PN synaptogenesis in postnatally developing *nr* cerebella. Whether BDNF/TrkB also affects dendritogenesis in normal PNs has been uncertain (47). We show here that blockage of BDNF/TrkB signaling by TrkB IgG does not interfere with dendritic growth and that a BDNF supplement fails to protect PN dendritogenesis while it is being suppressed by tPA+PL treatment. Despite the close general interrelationship between dendritic growth and synaptogenesis (25), these results suggest that BDNF/TrkB signaling may regulate PN synaptic formation via a mechanism independent of dendritic growth control. However, it remains unresolved whether tPA affects PF–PN synaptic plasticity and pathology by any of its several known proteolytic actions other than on BDNF, including plasmin-independent proteolytic cleavage at arginine 67 of the NR2B subunit of NMDA receptor (48). In addition, tPA also is reported to be a direct modulator of neurotransmission and synaptic plasticity by impacting glutamatergic and dopaminergic pathways (49).

Granule cell production of BDNF and its action on TrkB receptor-expressing PNs, as well as ultrastructural abnormalities in granule cell PF presynaptic vesicles and PN PSDs, as studied here in the *nr* mutant, are reminiscent of the many earlier analyses of cerebellar mutants that have demonstrated granule cell–PN interactions (50, 51). For example, in staggerer mice, the first described cerebellar mutant (52), a null mutation in the retinoid-related orphan nuclear receptor (53) leads to the failure of PNs to form dendritic spines and therefore to the failure of PF–PN synaptogenesis, with resultant massive death of the presynaptic granule cell neurons. In the opposite synaptic relationship, analyses of weaver and reeler mutants have established that granule cells and their parallel fiber axons are essential for PN dendritic maturation (25). Our present data provide plausible molecular mechanisms distinguishing dendritogenesis from synaptogenesis. A further search for possible influences in the *nr* mutant of granule cell neurons, which produce tPA and BDNF, on their PN partners is warranted.

A unique feature in *nr* PNs is that mitochondria begin to enlarge and round up on P9, with virtually all PNs so affected by P15 (10, 14), well before the onset of PN degeneration. The cristae within the enlarged mitochondria appear so "healthy" by routine electron microscopic criteria that for four decades it has been unknown whether these mitochondria are "super-normal" in an attempt to fight off the *nr* pathological process or are centrally involved in the impending cell-death mechanism. The only hints have been that some *nr* mitochondria, especially at older ages, undergo vacuolation and degeneration of cristae (42) or show some signs of incomplete degeneration in which the outer membrane partially or completely dissolves, occasionally accompanied by focal interruptions of the inner membrane (54). Mitochondrial swelling and defects in their outer membrane integrity can occur in multiple cell types in response to a range of necrosis- or apoptosis-inducing conditions (55), perhaps related to abnormal closure of VDAC pores in the mitochondrial outer membrane (56). Thus, the mitochondria

Downloaded at Palestinian Territory, occupied on December 16, 2021
www.manaraa.com

in young *nr* PNs share features of enlargement and rounding recognized in mitochondria engaged in mitoptosis (57, 58) but differ in that few of the mitochondria develop fragmented cristae or other degenerative changes except at much older ages. The *nr* mitochondrial phenotype may signify the onset of PN death, but it does not fit easily into the current standard classification of cell-death types (59, 60).

VDAC, a major anion channel in the mitochondrial outer membrane, is a multifunctional protein known to affect cell life and death (32, 56), although little information is available about molecular candidates controlling the fluctuating diameter of the VDAC channel pore. One prospective candidate is kringle 5, a peptide catabolite of plasminogen over-generated by the excess tPA. A reasonable hypothesis is that increased plasminogen-based kringle 5 binds specifically to brain VDAC, interferes with the regulation of intracellular Ca^{2+} and pH, and alters polarization of the mitochondrial membrane (37), finally leading to partial closure of this ion channel (61). Our findings of abnormalities in mitochondrial $\Delta\Psi$m, ATP production, and membrane integrity suggest that structural and functional disorder in the *nr* mitochondria and plasma membrane are central antecedents to PN cell death by a mechanism involving development of a VDAC1 channel disability, plausibly caused by excess kringle 5. Similar mitochondrial enlargement and rounding, with good retention of cristae, have been described in skeletal and cardiac muscle of VDAC1$^{-/-}$ mice (62), and mitochondrial enlargement without rounding has been described in skeletal muscle of VDAC3$^{-/-}$ mice (63).

Increases in tPA level and tPA/plasmin proteolytic activity also are found in other inherited cerebellar disorders. Lurcher (*Lc*), a dominant mutant disorder, results from an aberrant glutamate δ2 receptor in PN postsynaptic sites (64); and in *Lc*/$^{+}$;*tPA*$^{-/-}$ double mutants the elimination of endogenous tPA delays *Lc*/$^{+}$ PN death (41). Cerebellar tPA is increased in the mouse model of spinocerebellar ataxia type 1 before the PN loss but coincident with motor dysfunction (40). Weaver cerebellar neurons carry a mutant G protein-coupled inwardly rectifying K^{+} channel subunit 2 (Girk2) (65), and a tPA protease inhibitor, protinin, protects the neurons from cell death (66). Elimination of the high endogenous tPA in our *nr;tPA*$^{-/-}$ double mutants rescues most *nr* PNs examined at P40 and corrects their mitochondrial configurations, confirming excess tPA as a crucial molecule and, probably, abnormal mitochondria as key factors in the selective death of *nr* young PNs.

Because some PNs are lost at older ages in *nr;tPA*$^{-/-}$ double mutants, additional factors may be involved in this later-onset degeneration. Among many proteins likely to be changed in P65 *nr* cerebella, we have checked ankyrin (Ank), an adaptor linking various integral membrane proteins to the cellular cytoskeleton (67), whose deficiency leads to progressive loss of PNs in adult normoblastosis-mutant mice (68). We failed to identify Ank as a regulator of dendritic growth (Fig. 2), synaptogenesis (Fig. 4), mitochondria (Fig. 6), and cell death (Fig. 7) of young PNs but detected greatly down-regulated Ank1 in adult *nr* cerebellar cortices (Fig. S8). Further analysis is merited to establish if Ank1 deficiency and/or other factors influence the modest ongoing degeneration of adult *nr* PNs.

The *nr* gene is one of the few neurological mutant mouse genes that have evaded identification. In our previous work (14) we measured coding regions of *nr* candidate genes known through genome mapping to be located in a 1.4-cM segment of mouse chromosome 8 but failed to identify the *nr* gene. Although the present work provides important molecular and cellular mechanisms underlying *nr* PN development and survival, whether these mechanisms cause other mouse and/or human cerebellar diseases involving PN dysfunction and degeneration remains an open question. Additional genetic factors, particularly noncoding RNAs, merit consideration. For example, mutant U2 snRNA is responsible for massive cerebellar granule cell apoptosis without affecting the eight known coding genes in its immediate vicinity on mouse chromosome 11 (69).

In conclusion, the present study discloses mechanisms by which early tPA excess in the *nr* cerebellum leads to dendritic underdevelopment, abnormal synaptogenesis, mitochondrial malfunction, plasma membrane damage, and subsequent PN necrosis. PKCγ activation and MAP2 phosphorylation induced by excess tPA, whether endogenous in *nr* mice or injected in WT mice, suppress dendritic development of PNs. BDNF degradation by excess tPA/plasmin proteolysis impairs PF–PN synapses, evidenced both by ultrastructural quantification and by measurement of a postsynaptic marker. VDAC1 bound with unusually excessive amounts of the plasminogen catabolite kringle 5 alters mitochondrial morphology and $\Delta\Psi$m as well as plasma membrane integrity, resulting in young PN death by a necrosis mechanism, as evidenced by altered cell morphology without nuclear pyknosis or caspase activation, in agreement with earlier evidence on the appearance of PNs that are undergoing necrosis (34).

Materials and Methods

Animals. The *nr* mutation originally occurred in the Balb/cGr strain (9) and has been maintained by us congenic with the almost identical Balb/cByJ strain for >33 backcross generations. Animal preparation procedures were as previously described (14). For added details on mice and procedures, please refer to *SI Materials and Methods* and refs. 4, 27, and 70.

ACKNOWLEDGMENTS. We thank Monica L. Calicchio for guidance on laser capture microdissection, Veronica J. Peschansky for guidance on Neurolucida software, and Scott B. Berger for guidance on lentiviral particle concentration. This work was supported in part by National Institutes of Health Grant R33 CA103056, the Nancy Lurie Marks Family Foundation (R.L.S.), and the William Randolph Hearst Fund (J.L.).

1. Palay SL, Chan-Palay V (1974) *Cerebellar Cortex: Cytology and Organization.* (Springer, Berlin).
2. Llinás RR, Walton KD, Lang EJ (2004) *The Synaptic Organization of the Brain*, ed Shepherd GM (Oxford Univ Press, New York), 5th Ed, pp 271–309.
3. Rossi F, Tempia F (2006) Unravelling the Purkinje neuron. *Cerebellum* 5(2):75–76.
4. Kapfhammer JP, Gugger OS (2012) The analysis of Purkinje cell dendritic morphology in organotypic slice cultures. *J Vis Exp* 61(61):e3637.
5. Seidel K, et al. (2012) Brain pathology of spinocerebellar ataxias. *Acta Neuropathol* 124(1):1–21.
6. Kasumu A, Bezprozvanny I (2012) Deranged calcium signaling in Purkinje cells and pathogenesis in spinocerebellar ataxia 2 (SCA2) and other ataxias. *Cerebellum* 11(3): 630–639.
7. Fatemi SH, et al. (2012) Consensus paper: Pathological role of the cerebellum in autism. *Cerebellum* 11(3):777–807.
8. Stępień T, Wierzba-Bobrowicz T, Lewandowska E, Szpak G (2012) Morphological and quantitative analysis of cerebellar cortical cells in Alzheimer's disease. *Folia Neuropathol* 50(3):250–260.
9. Sidman RL, Green MC (1970) *"Nervous"*, a new mutant mouse with cerebellar disease. *In Les Mutants Pathologiques Chez L'animal. Leur Interpret pour la Recherche Biomedicale*, ed Sabourdy M (Centre National de la Recherche Scientifique, Paris), pp 69–79.
10. Landis SC (1973) Ultrastructural changes in the mitochondria of cerebellar Purkinje cells of nervous mutant mice. *J Cell Biol* 57(3):782–797.
11. Wassef M, Sotelo C, Cholley B, Brehier A, Thomasset M (1987) Cerebellar mutations affecting the postnatal survival of Purkinje cells in the mouse disclose a longitudinal pattern of differentially sensitive cells. *Dev Biol* 124(2):379–389.
12. De Jager PL, Harvey D, Polydorides AD, Zuo J, Heintz N (1998) A high-resolution genetic map of the nervous locus on mouse chromosome 8. *Genomics* 48(3):346–353.
13. Li J, Imitola J, Snyder EY, Sidman RL (2006) Neural stem cells rescue nervous Purkinje neurons by restoring molecular homeostasis of tissue plasminogen activator and downstream targets. *J Neurosci* 26(30):7839–7848.
14. Li J, et al. (2006) Purkinje neuron degeneration in nervous (nr) mutant mice is mediated by a metabolic pathway involving excess tissue plasminogen activator. *Proc Natl Acad Sci USA* 103(20):7847–7852.
15. Seeds NW, Williams BL, Bickford PC (1995) Tissue plasminogen activator induction in Purkinje neurons after cerebellar motor learning. *Science* 270(5244):1992–1994.
16. Friedman GC, Seeds NW (1995) Tissue plasminogen activator mRNA expression in granule neurons coincides with their migration in the developing cerebellum. *J Comp Neurol* 360(4):658–670.
17. Basham ME, Seeds NW (2001) Plasminogen expression in the neonatal and adult mouse brain. *J Neurochem* 77(1):318–325.

Downloaded at Palestinian Territory, occupied on December 16, 2021
www.manaraa.com

18. NINDS rt-PA Stroke Study Group (1995) Tissue plasminogen activator for acute ischemic stroke. *N Engl J Med* 333(24):1581–1587.
19. Dusart I, Flamant F (2012) Profound morphological and functional changes of rodent Purkinje cells between the first and the second postnatal weeks: A metamorphosis? *Front Neuroanat* 6(11), 10.3389/fnana.2012.00011.
20. He K-L, et al. (2011) Feedback regulation of endothelial cell surface plasmin generation by PKC-dependent phosphorylation of annexin A2. *J Biol Chem* 286(17): 15428–15439.
21. Barmack NH, Qian Z, Yoshimura J (2000) Regional and cellular distribution of protein kinase C in rat cerebellar Purkinje cells. *J Comp Neurol* 427(2):235–254.
22. Schrenk K, Kapfhammer JP, Metzger F (2002) Altered dendritic development of cerebellar Purkinje cells in slice cultures from protein kinase C gamma-deficient mice. *Neurosci* 110(4):675–689.
23. Kapfhammer JP (2004) Cellular and molecular control of dendritic growth and development of cerebellar Purkinje cells. *Prog Histochem Cytochem* 39(3):131–182.
24. Tabata T, et al. (2000) A reliable method for culture of dissociated mouse cerebellar cells enriched for Purkinje neurons. *J Neurosci Methods* 104(1):45–53.
25. Sotelo C, Dusart I (2009) Intrinsic versus extrinsic determinants during the development of Purkinje cell dendrites. *Neuroscience* 162(3):589–600.
26. Chauhan N, Siegel G (1997) Age-dependent organotypic expression of microtubule-associated proteins (MAP1, MAP2, and MAP5) in rat brain. *Neurochem Res* 22(6): 713–719.
27. Li J, et al. (2010) Nna1 mediates Purkinje cell dendritic development via lysyl oxidase propeptide and NF-κB signaling. *Neuron* 68(1):45–60.
28. Chen LJ, Wang YJ, Tseng GF (2010) Compression alters kinase and phosphatase activity and tau and MAP2 phosphorylation transiently while inducing the fast adaptive dendritic remodeling of underlying cortical neurons. *J Neurotrauma* 27(9): 1657–1669.
29. Mori A, et al. (1991) Site-specific phosphorylation by protein kinase C inhibits assembly-promoting activity of microtubule-associated protein 4. *Biochemistry* 30(38):9341–9346.
30. Carter AR, Chen C, Schwartz PM, Segal RA (2002) Brain-derived neurotrophic factor modulates cerebellar plasticity and synaptic ultrastructure. *J Neurosci* 22(4): 1316–1327.
31. Shoshan-Barmatz V, et al. (2010) VDAC, a multi-functional mitochondrial protein regulating cell life and death. *Mol Aspects Med* 31(3):227–285.
32. Shoshan-Barmatz V, Golan M (2012) Mitochondrial VDAC1: Function in cell life and death and a target for cancer therapy. *Curr Med Chem* 19(5):714–735.
33. Shoshan-Barmatz V, Ben-Hail D (2012) VDAC, a multi-functional mitochondrial protein as a pharmacological target. *Mitochondrion* 12(1):24–34.
34. Dusart I, Guenet JL, Sotelo C (2006) Purkinje cell death: Differences between developmental cell death and neurodegenerative death in mutant mice. *Cerebellum* 5(2):163–173.
35. Gonzalez-Gronow M, Ray R, Wang F, Pizzo SV (2013) The voltage-dependent anion channel (VDAC) binds tissue-type plasminogen activator and promotes activation of plasminogen on the cell surface. *J Biol Chem* 288(1):498–509.
36. Hiller S, et al. (2008) Solution structure of the integral human membrane protein VDAC-1 in detergent micelles. *Science* 321(5893):1206–1210.
37. Gonzalez-Gronow M, Kalfa T, Johnson CE, Gawdi G, Pizzo SV (2003) The voltage-dependent anion channel is a receptor for plasminogen kringle 5 on human endothelial cells. *J Biol Chem* 278(29):27312–27318.
38. Mannella CA, Kinnally KW (2008) Reflections on VDAC as a voltage-gated channel and a mitochondrial regulator. *J Bioenerg Biomembr* 40(3):149–155.
39. Chaabane W, et al. (2013) Autophagy, apoptosis, mitoptosis and necrosis: Interdependence between those pathways and effects on cancer. *Arch Immunol Ther Exp (Warsz)* 61(1):43–58.
40. Sashindranath M, et al. (2011) Compartment- and context-specific changes in tissue-type plasminogen activator (tPA) activity following brain injury and pharmacological stimulation. *Lab Invest* 91(7):1079–1091.
41. Lu W, Tsirka SE (2002) Partial rescue of neural apoptosis in the Lurcher mutant mouse through elimination of tissue plasminogen activator. *Development* 129(8):2043–2050.
42. Sotelo C, Triller A (1979) Fate of presynaptic afferents to Purkinje cells in the adult nervous mutant mouse: A model to study presynaptic stabilization. *Brain Res* 175(1): 11–36.
43. Haraguchi S, et al. (2012) Estradiol promotes Purkinje dendritic growth, spinogenesis, and synaptogenesis during neonatal life by inducing the expression of BDNF. *Cerebellum* 11(2):416–417.
44. Kline DD, Ogier M, Kunze DL, Katz DM (2010) Exogenous brain-derived neurotrophic factor rescues synaptic dysfunction in Mecp2-null mice. *J Neurosci* 30(15):5303–5310.
45. Furutani K, Okubo Y, Kakizawa S, Iino M (2006) Postsynaptic inositol 1,4,5-trisphosphate signaling maintains presynaptic function of parallel fiber-Purkinje cell synapses via BDNF. *Proc Natl Acad Sci USA* 103(22):8528–8533.
46. Hisatsune C, et al. (2006) Inositol 1,4,5-trisphosphate receptor type 1 in granule cells, not in Purkinje cells, regulates the dendritic morphology of Purkinje cells through brain-derived neurotrophic factor production. *J Neurosci* 26(42):10916–10924.
47. Bosman LW, et al. (2006) Requirement of TrkB for synapse elimination in developing cerebellar Purkinje cells. *Brain Cell Biol* 35(1):87–101.
48. Ng K-S, Leung H-W, Wong PT-H, Low C-M (2012) Cleavage of the NR2B subunit amino terminus of N-methyl-D-aspartate (NMDA) receptor by tissue plasminogen activator: Identification of the cleavage site and characterization of ifenprodil and glycine affinities on truncated NMDA receptor. *J Biol Chem* 287(30):25520–25529.
49. Samson AL, Medcalf RL (2006) Tissue-type plasminogen activator: A multifaceted modulator of neurotransmission and synaptic plasticity. *Neuron* 50(5):673–678.
50. Goldowitz D, Hamre KM (1998) The cells and molecules that make a cerebellum. *Trends Neurosci* 21(9):375–382.
51. Sajan SA, Waimey KE, Millen KJ (2010) Novel approaches to studying the genetic basis of cerebellar development. *Cerebellum* 9(3):272–283.
52. Sidman RL, Lane PW, Dickie MM (1962) Staggerer, a new mutation in the mouse affecting the cerebellum. *Science* 137(3530):610–612.
53. Hamilton BA, et al. (1996) Disruption of the nuclear hormone receptor RORalpha in staggerer mice. *Nature* 379(6567):736–739.
54. Berrebi AS, Mugnaini E (1988) Effects of the murine mutation 'nervous' on neurons in cerebellum and dorsal cochlear nucleus. *J Neurocytol* 17(4):465–484.
55. Vander Heiden MG, Chandel NS, Williamson EK, Schumacker PT, Thompson CB (1997) Bcl-xL regulates the membrane potential and volume homeostasis of mitochondria. *Cell* 91(5):627–637.
56. Vander Heiden MG, et al. (2000) Outer mitochondrial membrane permeability can regulate coupled respiration and cell survival. *Proc Natl Acad Sci USA* 97(9): 4666–4671.
57. Skulachev VP (2006) Bioenergetic aspects of apoptosis, necrosis and mitoptosis. *Apoptosis* 11(4):473–485.
58. Jangamreddy JR, Los MJ (2012) Mitoptosis, a novel mitochondrial death mechanism leading predominantly to activation of autophagy. *Hepat Mon* 12(8):e6159.
59. Weerasinghe P, Buja LM (2012) Oncosis: An important non-apoptotic mode of cell death. *Exp Mol Pathol* 93(3):302–308.
60. Galluzzi L, et al. (2009) Guidelines for the use and interpretation of assays for monitoring cell death in higher eukaryotes. *Cell Death Differ* 16(8):1093–1107.
61. Banerjee J, Ghosh S (2004) Interaction of mitochondrial voltage-dependent anion channel from rat brain with plasminogen protein leads to partial closure of the channel. *Biochim Biophys Acta* 1663(1-2):6–8.
62. Anflous K, Armstrong DD, Craigen WJ (2001) Altered mitochondrial sensitivity for ADP and maintenance of creatine-stimulated respiration in oxidative striated muscles from VDAC1-deficient mice. *J Biol Chem* 276(3):1954–1960.
63. Sampson MJ, et al. (2001) Immotile sperm and infertility in mice lacking mitochondrial voltage-dependent anion channel type 3. *J Biol Chem* 276(42):39206–39212.
64. Zuo J, et al. (1997) Neurodegeneration in Lurcher mice caused by mutation in delta2 glutamate receptor gene. *Nature* 388(6644):769–773.
65. Patil N, et al. (1995) A potassium channel mutation in weaver mice implicates membrane excitability in granule cell differentiation. *Nat Genet* 11(2):126–129.
66. Murtomäki S, Trenkner E, Wright JM, Saksela O, Liesi P (1995) Increased proteolytic activity of the granule neurons may contribute to neuronal death in the weaver mouse cerebellum. *Dev Biol* 168(2):635–648.
67. Bennett V (1992) Ankyrins. Adaptors between diverse plasma membrane proteins and the cytoplasm. *J Biol Chem* 267(13):8703–8706.
68. Peters LL, et al. (1991) Purkinje cell degeneration associated with erythroid ankyrin deficiency in nb/nb mice. *J Cell Biol* 114(6):1233–1241.
69. Jia Y, Mu JC, Ackerman SL (2012) Mutation of a U2 snRNA gene causes global disruption of alternative splicing and neurodegeneration. *Cell* 148(1-2):296–308.
70. Li J, Pelletier MR, Perez Velazquez JL, Carlen PL (2002) Reduced cortical synaptic plasticity and GluR1 expression associated with fragile X mental retardation protein deficiency. *Mol Cell Neurosci* 19(2):138–151.

Downloaded at Palestinian Territory, occupied on December 16, 2021

www.manaraa.com